

# Robustness Analysis for Droplet-Based Microfluidic Networks

Gerold Fink *Student Member, IEEE*, Andreas Grimmer *Member, IEEE*, Medina Hamidović, Werner Haselmayr *Member, IEEE*, and Robert Wille *Senior Member, IEEE*

**Abstract**—Microfluidic networks can be applied to droplet-based *Lab-on-a-Chip* devices, where droplets are used to confine samples which flow through closed microchannels along different paths in order to execute (bio-)chemical experiments. In order to allow this routing of droplets, the design of the microfluidic network has to be precisely defined and afterwards fabricated. However, neither the fabrication process nor the applied materials and components are perfect and, therefore, the fabricated microfluidic device frequently contains defects (produced by fabrication tolerances, properties of the used material, or fluctuation of supply pumps). Those may have a severe impact on the behavior of the microfluidic network and can even render the network useless. Furthermore, these defects complicate the design process, which eventually results in a “trial-and-error”-approach causing high costs with respect to time and money. Consequently, designers want to anticipate how robust their design is against those defects. This work, for the first time, describes how these defects can be abstracted, which eventually allows to evaluate the robustness already in the design process. We additionally introduce models considering single and multiple defects as well as corresponding methods for their analysis. Evaluations on a microfluidic network which is used to screen drug compounds confirm that the resulting robustness analysis indeed provides designers with a simple metric to decide how sensitive their design is against defects. The models and methods proposed in this paper are grounded on the established one-dimensional analysis model.

**Index Terms**—Droplet microfluidics, microfluidic networks, robustness

## I. INTRODUCTION

Microfluidics deals with the manipulation and control of small amounts of fluids, usually in the order of a few micro- to pico-liters, and is frequently applied for *Lab-on-a-Chip* devices. Especially, the microfluidics platform where *droplets* are used to confine certain samples allows to conduct a broad range of chemical and biochemical experiments [1] and is a powerful high throughput platform [2]. In this platform, such droplets flow through closed microchannels (called channels in the following) inside a second immiscible fluid (called continuous phase) which acts as a carrier for the droplets and is driven by pumps. In order to manipulate and route droplets inside a microfluidic network *passive hydrodynamic effects* can be exploited and, thus, no active components such as expensive valves or control logics are required [3], [4]. Besides that, microfluidic devices can be realized rather easily using a base material such as *Polydimethylsiloxane* (PDMS) and fabrication techniques such as soft-lithography, 3D-printing, or milling techniques [5].

However, the passive effects mentioned above depend on various factors such as the channel dimensions, the applied

pressures, the used fluids, and even on the positions of the droplets inside the network. Furthermore, neither the fabrication nor the used materials are perfect, i.e., the fabrication accuracy is limited by tolerances, or soft materials, such as PDMS, deforms under pressure or swells for some organic solvents<sup>1</sup>. Finally, in order to supply the network with particular fluids, peristaltic and/or syringe pumps are used which may lead to fluctuations in the respectively generated supplied force (e.g. pressure drops in case of peristaltic pumps or changes in the volumetric flow rate in case of syringe pumps). Eventually, this will significantly affect the flow rates in the channels and, hence, may have a severe impact on the overall behavior of the microfluidic network. Furthermore, those defects complicate the design process as they are hard to be anticipated—resulting in a “trial and error” design approach.

At the same time, it certainly is possible to design a microfluidic network in a fashion which is *robust* against those defects, e.g., by adjusting the channel geometries so that, even if certain defects occur, the correct functionality of the device is still guaranteed. However, thus far, it is not possible to evaluate the robustness of a design against such defects for a microfluidic network. Consequently, many designs are just realized without really knowing the chances of actually getting a working device realized.

In other technologies like digital microfluidic biochips (utilizing electrowetting on dielectric) or flow-based biochips (utilizing valves), reliability, fault-tolerance, and error recovery have been investigated in detail (see e.g. [10], [11], [12]). In this work, for the first time, we are addressing this issue for microfluidic networks with passive droplet routing. To this end, we

- discuss what defects usually may occur and how to consider them already during the design process,
- propose particular *robustness models* which give designers the possibility to evaluate their microfluidic design for its robustness against any of those defects, and
- introduce corresponding methods to analyze the robustness of a microfluidic network with respect to these models.

The resulting models and methods are grounded on the one-dimensional (1D) analysis model [13], which is commonly used for designing microfluidic networks and is based on the duality between electrical and microfluidic networks.

<sup>1</sup>That these defects likely occur in fabricated devices, is discussed in previous evaluations such as [6], [5], [7], [8], [9].

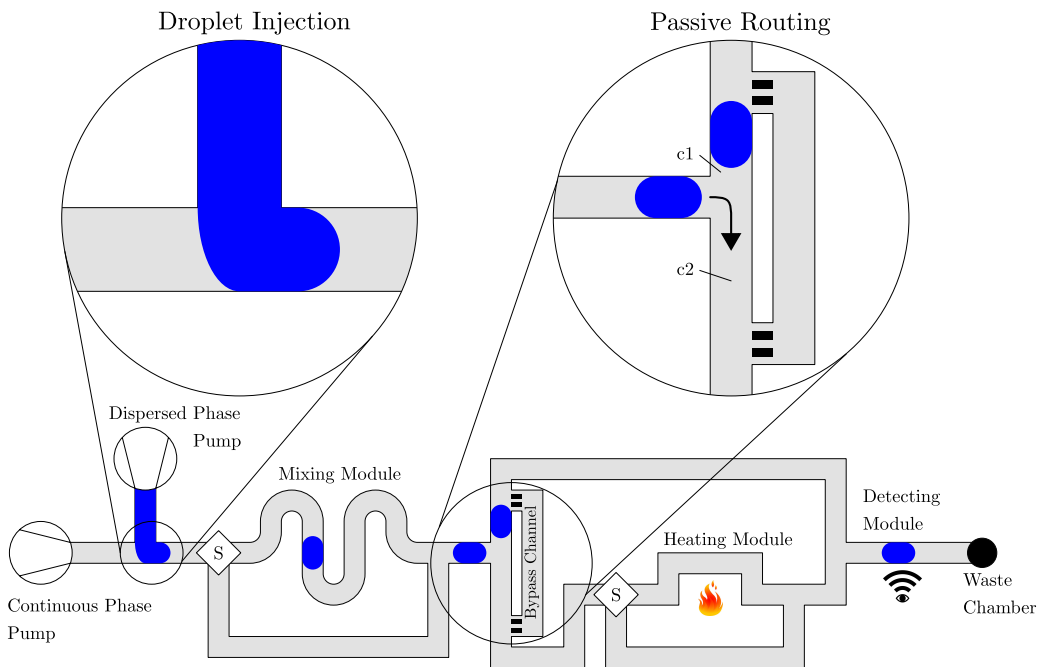


Fig. 1: Sketch of a microfluidic network.

The robustness models and methods are demonstrated on a microfluidic network [9] which is used to screen drug compounds. Those evaluations show that the resulting approach enables designers to evaluate the robustness of their designed microfluidic device prior to fabrication. By this, it provides designers with a simple metric to decide how sensitive their design is against defects and, in case the design is considered not robust enough, to correspondingly adjust it prior to fabrication. Furthermore, the models proposed in this work presents the basis for design methods which inherently obtain robust designs.

The remainder of this paper is structured as follows: In the next section, we review the basic principles of microfluidic networks as well as the considered model of microfluidic channels and droplets. Furthermore, we introduce a microfluidic network which we use as running example throughout this work. Afterwards in Sec. III, we investigate possible defects in microfluidic devices. In Sec. IV, we introduce different robustness models, which are able to consider such defects. The analysis of the robustness models as well as the simulation framework which is exploited for this analysis are described in Sec. V. Finally, the results obtained with these models and methods are presented and discussed in Sec. VI before the paper is concluded in Sec. VII.

## II. BACKGROUND

To keep this work self-contained, this section first briefly reviews microfluidic networks as well as the underlying 1D analysis model. Afterwards, the microfluidic network [9] is introduced which is used to illustrate the concepts of the proposed robustness analysis in the remainder of this paper. For a more detailed treatment on the issues reviewed here, we refer to the respectively provided references.

### A. Microfluidic Networks

The major components of a microfluidic network are sketched in Fig. 1. Here, pumps produce a flow of the continuous phase and a flow of the dispersed phase. When both phases meet, e.g., in a T-junction, droplets are formed [1] and injected into the network (as highlighted in the left detail of Fig. 1). Afterwards, the droplets are routed through different components, e.g., a mixing module, a heating module, and a detecting module which are all used to process different operations. More precisely, the mixing module is used to mix the reagents inside a droplet, while the heating module increases the temperature of the droplets and, by this, triggers a reaction between these reagents. Finally, the detecting module is used to screen the droplets in order to evaluate the reaction of the reagents.

In order to control which paths are taken, a passive routing mechanism is employed which relies on bifurcations (highlighted in the right detail of Fig. 1). Here, the successor channels (named  $c_1$  and  $c_2$  in the figure) realize different hydrodynamic resistances, which are mainly defined by the channel geometries (i.e. the smaller the diameter and/or the longer the channel, the higher the resistance) and viscosity of the continuous phase.<sup>2</sup> A droplet will always enter the channel with the lowest resistance [14], [15] or, in other words, with the highest instantaneous flow rate, i.e., channel  $c_1$  in the considered case (called the default successor). However, if the droplet should enter the other channel, again hydrodynamic effects can be exploited. In fact, the presence of a droplet inside a channel increase the hydrodynamic resistance of the channel e.g. through their viscosities, droplet size, and

<sup>2</sup>A bypass channel [14] connects the endpoints of the two successor channels. This bypass cannot be entered by any droplet and is used to make the droplet routing only dependent on the resistances of the successors.

geometry as studied e.g. in [16], [17], [18]. This has the effect that, when the network is properly designed, the resistance of the default successor becomes larger than the resistance of the non-default successor, i.e., a droplet may temporarily block the default successor for following droplets. This allows to route a second, closely following, droplet into the non-default successor (as shown in the right detail of Fig. 1).

These concepts allow to route droplets along arbitrary paths through a microfluidic network. More precisely, if the actually considered droplet is supposed to take a non-default successor at any bifurcation in the network, it has to make sure that another droplet arrives before and flows through the default successor (i.e. this droplet temporarily blocks the default successor for closely following droplets) [19]. Corresponding methods for determining proper droplet sequences as well as physical realizations of the respectively needed droplet-on-demand functionality have been proposed in [20], [21] and [22], [23], [24], respectively. Overall, this allows for the realization of various experiments and applications by the microfluidic network.

### B. 1D Analysis Model

The concepts reviewed above can be physically described using, e.g., the 1D analysis model covered in [13], [25]. This model exploits the fact that, in microfluidic devices, the flow of the fluids usually occurs at low Reynolds numbers (i.e. the ratio of inertial to viscous forces is rather small due to the small channel sections and relatively small flow rates). Hence, inertial effects such as gravity, separation, secondary flow, and turbulence are negligible and the pumps produce a fully developed and laminar flow [8]—allowing to describe the flow using *Hagen-Poiseuille's law* [26], [13]

$$\Delta P = Q \cdot R, \quad (1)$$

where  $Q$  is the volumetric flow rate,  $\Delta P$  the pressure gradient, and  $R$  the hydrodynamic resistance. Note that a duality between Hagen-Poiseuille's law in the microfluidic domain and Ohm's law in the electrical domain exists. In fact, all concepts and laws of the 1D model are equivalent to the corresponding laws for electrical circuits which is why this description is also common in the respective literature [18], [27], [13].

Each channel poses a hydrodynamic resistance  $R$  against the flow, which depends on the geometry of the channel but also on the dynamic viscosity of the continuous phase  $\mu_c$ . For rectangular channels with width  $w$ , height  $h$ , and length  $l$  as well as a section ratio  $h/w < 1$ , the hydrodynamic resistance is defined by [17]

$$R = \frac{a \mu_c l}{w h^3}, \quad (2)$$

where  $a$  denotes a dimensionless parameter defined as

$$a = 12 \left[ 1 - \frac{192 h}{\pi^5 w} \tanh \left( \frac{\pi w}{2 h} \right) \right]^{-1}. \quad (3)$$

Furthermore, not only channels pose a resistance but, as reviewed above, also the presence of droplets inside a channel. When droplets have a minimum distance of typically a few

channel sections, their flow perturbations do not interact anymore [25], which allows to model each droplet as an additional resistance. The work in [16] proposed a rule that each droplet with length  $L_d$  increases the resistance of the segment of the channel it occupies by 2–5 times, when the Capillary number and the ratio between the dispersed and continuous phase are small (i.e.  $Ca < 0.01$  and  $\frac{\mu_d}{\mu_c} < 0.1$ ). In the following, we assume a factor 3, i.e., the hydrodynamic resistance of a droplet can be described by

$$R_d = \frac{3 a \mu_c L_d}{w h^3}. \quad (4)$$

A channel containing  $n$  droplets has, therefore, a total resistance of

$$R^* = R + n R_d. \quad (5)$$

Finally, the pumps produce a force which can be a constant flow rate  $Q_{in}$  (e.g. by using syringe pumps) or a pressure gradient  $\Delta P_{in}$  (e.g. by using peristaltic pumps). The following two rules allow to describe the distribution of the flow rates/pressure gradients produced by the pumps and are similar to Kirchhoff's laws in the electrical domain:

- The sum of flow rates in a microfluidic network meeting at any point is zero.
- The sum of directed pressure gradients around any closed loop in a microfluidic network is zero.

These two laws allow to setup an equation system which can be used to determine the flow state for all channels. The flow state of a channel determines the *instantaneous* speed of the continuous phase by dividing the flow rate  $Q$  with the cross-section of the channel  $A = w \cdot h$ . Using this speed of the continuous phase and multiplying it with a slip factor  $\alpha$ , allows to determine the instantaneous speed of the droplets. However, the flow state as well as the speed of the droplets change as soon as (1) a new droplet is injected, (2) any of the droplets enters another channel, or (3) any droplet exits the microfluidic network, which requires to adapt the equation system (i.e. add, move, or remove the resistance of the droplets) and to re-solve it.

The obtained flow state can also be used to check pressure gradients whether or not they exceed the Laplace pressure, which e.g. would cause a droplet to be squeezed through a gap. The Laplace pressure is defined by [28]

$$\Delta P_{Lap} = \gamma \left[ \left( \frac{2}{w_{gap}} + \frac{2}{h} \right) - \left( \frac{1}{r_d} + \frac{2}{h} \right) \right], \quad (6)$$

where  $\gamma$  is the interfacial tension,  $w_{gap}$  the width of the gap, and  $r_d$  the droplet radius.

By all this, the behavior of a microfluidic network and the droplets in it can be described, as confirmed in previous evaluations such as [8], [9], [6], [5], [7], [13]. Moreover, the model has already been successfully applied in simulation (see, e.g., [29]) or design automation (see, e.g., [30], [31], [32]). To ease the user, also corresponding simulation approaches are available, e.g., in [27].

### C. Considered Running Example

In order to demonstrate the robustness analysis of microfluidic networks proposed in this work, we consider the microfluidic network introduced in [9] as a running example. This network realizes trapping wells, which are able to trap, merge, and mix droplets from two different droplet streams. With the help of these trapping wells, the network is able to screen drug compounds that inhibit the tau-peptide aggregation. Because the reagents cannot be premixed for real-time monitoring, the reaction needs to be triggered on demand, which is achieved by the trapping wells. Overall, this allows to significantly reduce the sample consumption volume by a factor of 100 compared to the approach with traditional 96-well plates. Moreover, the resulting network allows to reduce the reaction time from 2 hours to several minutes.

Details of the design are provided in Fig. 2 which focus on a single trapping well pair (the network itself has multiple trapping wells which are connected in series). As already mentioned, the trapping well pair is connected with two different droplet streams, where the droplets transport two different reagents. In Fig. 2 these streams are represented by the upper path and the lower path, which are marked by blue and red arrows, respectively.

When a droplet flows along the path of a stream, it reaches the entrance of the corresponding trapping well (i.e. point  $P_1$  or  $P_4$ ). If the trapping well does not contain a droplet yet, the droplet flows into the trapping well, because the flow rate of the bypass channel is smaller than the flow rate into the trapping well, i.e.,  $Q_{c2} > Q_{c5}$  or  $Q_{c7} > Q_{c10}$ . Furthermore, a trapped droplet must not be squeezed through the gaps behind the trap and, therefore, the pressure drops  $P_2 - P_3$  and  $P_5 - P_6$  must not exceed the Laplace pressure. Similar, the droplet must not be squeezed into the other trapping well, which implies that the pressure drop  $|P_2 - P_5|$  must not exceed the Laplace pressure as well. Droplets which reach the entrance of an already occupied trapping well should be routed into the bypass channel towards the next trapping well, which is only possible, if the flow rate of the bypass channel is larger than the flow rate into the trapping well, i.e.,  $Q_{c5} > Q_{c2}$  or  $Q_{c10} > Q_{c7}$ . This is achieved by the trapped droplet, which blocks the downstream gaps of the traps and, therefore, reduces the flow rate into the trapping well drastically. As soon as two droplets are contained inside two connected trapping wells, they begin to merge and their reagents start to mix and react.

How to efficiently design (and, at the same time, satisfy all these constraints) as well as how to realize such a network is described in previous works [9], [29]. In the following, we use this network as an example for illustrating how to analyze robustness of this design against defects.

### III. DEFECTS IN MICROFLUIDIC NETWORKS

After a design of a microfluidic network is obtained, the next step is usually the fabrication process. In an ideal scenario, i.e. under perfect fabrication conditions and using perfect materials as well as pumps, a correspondingly obtained physical realization of the network would show exactly the same behavior as considered before using the physical description (or

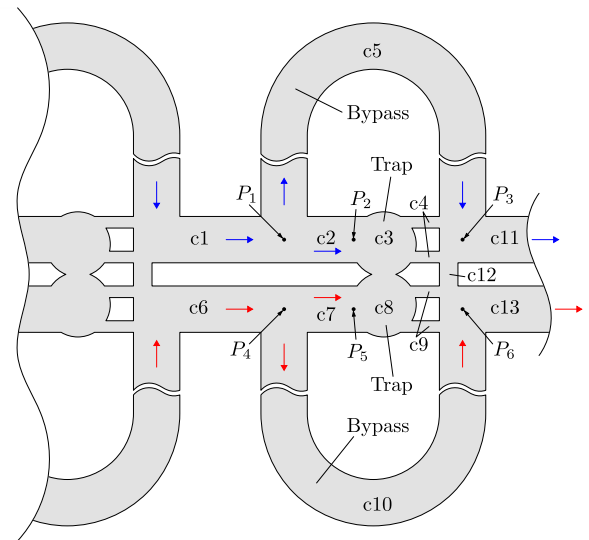


Fig. 2: Trapping wells as proposed in [9].

a corresponding simulator). However, neither the fabrication process nor the respectively used materials and pumps are perfect. In fact, the following defects are frequently observed in fabricated microfluidic devices:

- **Fabrication tolerances:** Depending on the fabrication process (e.g. soft-lithography techniques, 3D-printing, milling, or others), different fabrication tolerances occur [8]. This may lead to fabrication errors since the microfluidic network is eventually not as exactly fabricated as specified.
- **Pressure induced deformation and swelling of PDMS:** PDMS is the most common material used for producing prototypes of microfluidic networks due to its properties (PDMS allows for a rapid and low-cost fabrication, is biocompatible for many experiments, and is transparent) [5]. Despite these advantages, however, PDMS may deform under pressure-driven flows, which eventually affects the flow rates and pressure drops. These deformation effects have been theoretically and experimentally analyzed (a comprehensive overview is provided in [5]). Furthermore, some organic solvents (e.g. hexadecane, dichloromethane, and toluene) may swell the PDMS as well. For example, the experiments in [7] observe changes of up to 20% in the channel width due to swelling.
- **Fluctuation of supplying pumps:** In order to supply the network with the required continuous and dispersed phase, pumps are installed at the network boundaries. However, these pumps are not ideal and can fluctuate in their supplied force, e.g., pressure or volumetric flow rate. Such fluctuations affect the flow rates in all channels and may have an impact on the behavior of the microfluidic network.

The first two effects lead to geometry changes of the channels, which affect the flow rates and pressure drops in the network. The last effect directly influences these values. As a result, such defects may have a severe impact on the behavior of the device. Accordingly, designers may want to anticipate those

defects already in the design process and, if possible, derive a design which works as *robust* as possible with respect to these defects.

#### IV. ROBUSTNESS OF MICROFLUIDIC NETWORKS

In the previous section, we discussed different physical defects and how they could lead to erroneous behavior of the microfluidic network. Thus far, none of these potential defects are considered in the design process. This is a significant disadvantage since those defects are likely to occur (as discussed in previous evaluations such as [8], [9], [6], [5], [7]) and, then, will probably lead to an erroneous behavior—thus rendering the fabricated device useless. At the same time, it is clearly possible to design a microfluidic network in a *robust* fashion, e.g., by specifying the channel geometries in a way so that, even if certain amounts of fabrication defects, PDMS deformation and swelling as well as fluctuation of supply pumps occur, the desired behavior of the microfluidic network is still guaranteed. However, such considerations are not possible yet, because so far no method nor proper models for analyzing the robustness of a microfluidic network exist.

In the following, we address this issue. To this end, we first describe the objectives of an according robustness analysis. Afterwards, we propose two robustness models, which allow to explicitly quantify the resulting robustness—eventually yielding a metric defining the robustness of a microfluidic network. This is then used as basis for the proposed robustness analysis described in the following section.

##### A. Objectives

A microfluidic network is always designed in a way that it realizes an intended behavior or a specific task. Obviously, robustness analysis is to find out how much defects in a microfluidic network can jeopardize this behavior or the tasks to be conducted. To this end, the designer first has to define what is important for the desired behavior/tasks. Here, several objectives may exist such as

- the ratio between two flow rates must have a certain value,
- a droplet has to follow a desired path inside a microfluidic network,
- a droplet has to stay inside a trap and must not be squeezed through any gap, or
- the time a droplet needs to pass a specific channel must be beneath/above a given value.

Obviously, these objectives have to be satisfied by the initial design, i.e., the ideal design without defects, which serves as starting point for the robustness analysis. Then, the goal is to check whether defects, as described in Sec. III, have an effect to any of the objectives. This can be done by assuming those defects, i.e., changing the channel geometry or imposing fluctuations in the supply of the pumps, and determining whether the objectives are still satisfied. If this is the case, the design is robust against the assumed defects; otherwise it is not. However, since of course an infinite number of combinations of defects can be assumed in general, the definition of corresponding models is required. This is provided next.

##### B. Robustness Models

The number of defects which may occur in a microfluidic network is infinite. Therefore, in order to analyze the robustness of an entire microfluidic network design, corresponding *robustness models* are required. The main idea is thereby to abstract from the actual defects (as done for conventional integrated circuits, e.g., by fault models for testing [33], [34] or by models for robustness [35], [36], [37]).

For the microfluidic networks considered here, this can easily be done since all defects reviewed before in Sec. III can be described by

- changes in the dimensions of a channel (i.e. changes in the channel's length, width, and height) or
- changes in the forces supplied by the pumps (i.e. changes in the pressure and/or the volumetric flow rate).

Those changes can easily be imposed to the initially given design—both, in absolute as well as relative terms. This leaves the question where and how many defects shall be considered. To this end, we propose two types of robustness models in the following.

- *Single-Defect-Model*: This model assumes that the microfluidic network only contains a single defect of a particular channel or pump and, thus, assumes all other channels or pumps are defect-free. Therefore, it considers a single change in either one of the three dimensions of a channel (i.e. the channel's length, width, and height) or a defect in the supplied force of a pump (i.e. the pump's pressure and volumetric flow rate). The aim of this model is to state the minimal and maximal change a single defect can cause without harming any of the network's objectives. As a result, a network with a single defect is considered robust according to the single-defect-model, when this defect lies inside its corresponding minimal/maximal limits. Moreover, a consideration of single defects may also provide valuable information concerning the robustness of a network for multiple defects (i.e., defects which occur simultaneously), like it is the case in other domains such as the *Automatic Test Pattern Generation* for electronic circuits [38], [39].

**Example 1.** Consider the channel  $c_5$  from the running example introduced in Sec. II-C and illustrated in Fig. 2. Furthermore, assume that the ideal (i.e. defect-free) height of this channel is  $h_{c_5} = 60\mu\text{m}$  and the minimal defect as well as the maximal defect are determined by the values  $\Delta_{\min}(h_{c_5}) = 0.783$  and  $\Delta_{\max}(h_{c_5}) = 1.691$ , respectively. Then, this network still satisfies its objectives even if defects reduce the channel height to a value of  $h_{c_5,\min} = h_{c_5} \cdot \Delta_{\min}(h_{c_5}) = 46.98\mu\text{m}$  or increase it to a value of  $h_{c_5,\max} = h_{c_5} \cdot \Delta_{\max}(h_{c_5}) = 101.46\mu\text{m}$ . That is, the network is robust according to the single-defect-model (assuming a defect affecting the height of channel  $c_5$ ), as long as this defect does not exceed these limits. Obviously, the more those limits differ from the initial value the better the robustness of the network. Similarly, the robustness for width and length as well as for other channels and pumps can be described.

The robustness with respect to the single-defect-model can either be assessed for all channels/pumps of the microfluidic network or only on those which are specified by the designer. Hence, this model is a good choice, when the designer wants to know how sensitive the network is with respect to a single channel dimension or pump. However, it does not consider multiple defects occurring simultaneously (such as PDMS swelling which affects multiple/all channels). As a result, a network which is robust according to the single-defect-model does not necessarily have to be robust against multiple occurring defects. This issue is addressed by the next robustness model.

- **Multi-Defect-Model:** This model assumes that multiple defects occur simultaneously in the microfluidic network. Therefore, it considers defect combinations of channels and pumps, where it is also possible that multiple defects cancel each other out. The model considers defects on all three dimensions (i.e. length, width, and height) of all channels as well as defects on the supply force of all pumps. Compared to the single-defect-model, where the amount of defects grows linearly with the number of channels/pumps, the amount of different defect combinations in the multi-defect-model grows exponentially with the number of channels/pumps. As a result, it is very difficult to consider all these defect combinations—even for small networks. Moreover, all defects affect each other and are hard to decouple, which makes it nearly impossible to define minimal/maximal limits for each channel/pump as in the single-defect-model.

To overcome this problem, the model proposed here takes another approach and does not state the minimal/maximal defect limits of all possible combinations (which is infeasible anyway), but considers multiple defects according to a normal Gaussian distribution (assuming a certain standard deviation). The multi-defect-model now allows to determine how likely it is for the network to fulfill the desired objectives, when all defects are based on this normal Gaussian distribution with a certain standard deviation. The standard deviation can be adjusted by the designer and is usually chosen in such a way that it matches the standard deviation of the fabrication process or the fluctuation of the pumps. This value can also be adjusted individually for each channel/pump, which may give more accurate results. Therefore, it is possible to make a statement about, how likely it is to get a network with the intended behavior after the manufacture. Eventually this yields a robustness metric of much higher quality than the single-defect-model, because multiple defect combinations are considered and, hence, works as suitable compromise between efficiency and accuracy.

**Example 2.** Consider again the running example from above and let's assume the analysis of the network according to the multi-defect-model is based on defects determined by a normal Gaussian distribution and a standard deviation of  $\sigma = 0.15$ . Then, this network has a

*robustness of  $p_{\text{Success}} = 93.35\%$ <sup>3</sup>, i.e., there is a 93.35% chance that a network fabricated based on the given specifications still satisfies the objectives even if multiple defects (defined according to a normal Gaussian distribution) within the standard deviation occur. Obviously, the larger this probability, the more robust is the microfluidic network. If the designer manages to determine a design with  $p_{\text{Success}} = 100\%$  for a standard deviation that is in-line with his/her respective standard deviation of the fabrication process and pump fluctuations, there is a good chance that the design always can be fabricated so that the desired behavior is employed.*

These considerations eventually provide a definition of the robustness of a microfluidic network: A corresponding network is considered robust under the respectively applied model, if changes in the channel geometries and/or pump forces (within a particular interval or standard deviation) still yields the desired behavior, i.e., the satisfaction of the considered objectives summarized above. The fact whether single or multiple defects are considered, the size of the interval or value of standard deviation as well as the number of satisfied objectives obviously is an indication about the quality of the robustness. How this can be efficiently analyzed is addressed in the next section.

## V. ANALYZING ROBUSTNESS

Having the foundations from above, we now can describe how the robustness of a given microfluidic network can be analyzed. As stated above, all discussed defects can be described by changes in the dimensions of a channel or by changes in the forces supplied by the pumps. To analyze their effect on the objectives of a network, the physical description reviewed in Sec. II-B as well as corresponding simulators (available, e.g., in [27]) can be utilized. In the following, we are describing a possible approach. To this end, we first present a brief overview of the used simulator and its working principles. Afterwards, the analysis scheme is outlined in detail. Please note that the final result of the analysis does not yield information on whether a defect really occurs in a fabricated network, but provides crucial information on whether the resulting device would withstand such defects (i.e., whether the resulting device would be robust against such defects).

### A. Simulator

In the proposed robustness analysis, we are utilizing the simulator proposed in [27] which is based on the 1D model reviewed in Sec. II-B. The simulator captures the behavior of a microfluidic network in five steps:

- 1) **Initialization:** In order to simulate a droplet-based microfluidic network, the designer has to initialize the simulation first. This means, the designer has to provide the following specifications:
  - Dimensions of all channels (i.e. their length, width, and height)

<sup>3</sup>Note that how this value is determined is described later in Sec. V-B2.

- Structure of the network (i.e. how the channels/pumps are connected with each other)
- Pressure or volumetric flow rate of the supply pumps
- Properties of the continuous and dispersed phase (viscosity, density, interfacial-tension)
- Droplet volumes and their injection times

After passing these specifications to the simulator, the actual simulation process can start and the following steps are performed in a loop.

- 2) *Compute flow state*: The simulator converts the channels and droplets into their equivalent hydrodynamic resistances and derives a linear equation system that captures the physical behavior as described in Sec. II-B. This equation system is then used to determine the instantaneous flow state (i.e. pressure drops and flow rates in all channels) inside the microfluidic network. With the obtained flow rates, it is possible to determine the droplet velocities, which are required for the next step.
- 3) *Compute next event-time*: An event is basically an incident, which changes the current flow state of the microfluidic network and can be triggered by
  - injecting a droplet into the network,
  - a droplet flowing into another channel, or
  - a droplet leaving the network.

Therefore, the simulator computes the time when the next event gets triggered, which is achieved by using the previously computed droplet velocities.

- 4) *Update system state*: The simulator updates the system state (i.e. droplet positions and their resistances in the channels) accordingly to the occurred events and droplet velocities.
- 5) *Termination condition*: If a termination condition is reached (e.g. all droplets left the network), the simulation stops, otherwise, the simulator continues with Step 2 and computes the flow state again. Because the simulator stores each system state at every time step, the paths of the droplets as well as the flow states can be easily obtained.

Overall, after initializing the simulator, it always re-calculates the flow state of the network, when the old one becomes invalid due to an occurrence of an event. A huge advantage of such an event-based simulation compared to CFD-Simulations tools like Comsol Multiphysics, Ansys, or OpenFoam (such as proposed in [40], [41]) is that the computational time is much lower and, therefore, allows to simulate even large microfluidic networks in negligible runtime—yielding an ideal compromise between efficiency and accuracy. In fact, works such as [29] showed that the 1D-model provides a sufficient abstraction of the real world and can be used to describe the behavior of a microfluidic network (even if some details which can be provided by CFD have to be ignored for this purpose). Moreover, the small computational time is also helpful, when a large amount of simulations have to be conducted (as it is required in the robustness analysis considered here), which would be computationally infeasible using CFD simulations.

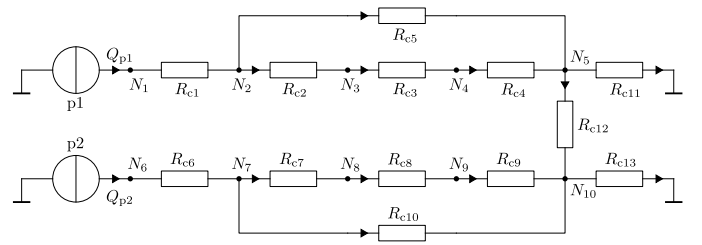


Fig. 3: Equivalent electrical network

### B. Determination the Robustness

Using the simulator as well as the models reviewed and introduced above, respectively, the robustness of a microfluidic network can now be determined by taking the corresponding design, converting it into the proper model to be used by the simulator, and iteratively employ changes on the design (according to the model) as well as observe how those changes affect the objectives. In the following, we describe the required steps in general and exemplary illustrate this using the running example reviewed before in Sec. II-C.

First, the structure of the network and the dimensions of the channels are converted into the 1D model. To this end, each channel of a network is represented with its hydrodynamic resistance. Furthermore, the start and end points of each channel are represented by nodes. These nodes and the information about what channels are connected to them are passed to the simulator—defining the structure of the network.

**Example 3.** Consider again the running example as shown in Fig. 2. To analyze its robustness, we first convert all channels into the 1D model. This is sketched in Fig. 3, where the respective hydrodynamic resistances and the resulting structure of the network are provided in terms of an electrical circuit (see Sec. II-B). Note that also trapping wells (i.e. c3 and c8) can be modeled by hydrodynamic resistances, however, additionally the Laplace pressures between the entrance and exit of the traps have to be checked, in order to determine if a droplet gets squeezed through any gaps. Moreover, we observed from the results in [9] that the volumetric flow rates at the input channels (i.e. c1 and c6) of the trapping well don't change, but rather stay constant during time. Therefore, this can be modeled in the 1D analysis model by using two current sources (i.e. p1 and p2). The initial dimensions of the channels are provided in Tab. I, which are taken from [9]<sup>4</sup>.

After defining the structure and the channel dimensions of a network, the fluid properties as well as the supply forces of the pumps, i.e., the pressure drops and/or volumetric flow rates of each pump, have to be defined. Moreover, the two

<sup>4</sup>Please note that we combined the two channels/gaps behind each trap into one channel (i.e. c4, c9), which does not make any difference in the 1D analysis model, because these channels are not meant to be passed by a droplet. Therefore, we considered this by half the length of the channels c4 and c9, respectively. Furthermore, note that the the input (i.e. c1 and c6) and output channels (i.e. c11 and c13) are not included in the robustness analysis, since they are only used to guide the droplets towards/away from the trapping well and, thus, work as a predefined start/end point. Therefore, they are modeled as very long channels with a large hydrodynamic resistance so they don't affect the behavior of the trapping well.

TABLE I: Channel dimensions

	Channels												
	c1	c2	c3	c4	c5	c6	c7	c8	c9	c10	c11	c12	c13
Length [ $\mu\text{m}$ ]	2000	109	170	72/2	4000	2000	109	170	72/2	4000	2000	50	2000
Width [ $\mu\text{m}$ ]	120	120	170	25	120	120	120	170	25	120	120	50	120
Height [ $\mu\text{m}$ ]	60	60	60	60	60	60	60	60	60	60	60	60	60

TABLE II: Fluid properties

	Fluid Settings	
	F1	F2
$\mu_c$ [Pa s]	4.565e-03	9.3e-03
$\mu_d$ [Pa s]	1e-03	1e-03
$\rho_c$ [ $\text{kg}/\text{m}^3$ ]	913	913
$\gamma$ [N/m]	0.042	0.042

droplet streams have to be specified, i.e., the droplet volumes and at which times the droplets appear at the corresponding input channels.

**Example 4.** For our running example, we can obtain these required values from the results reported in [9]. Accordingly, the volumetric flow rates of the pumps are identically set to  $Q_{p1} = Q_{p2} = 4,6914 \frac{\mu\text{l}}{\text{min}}$ . Moreover, the volumes of all droplets are defined by  $V_{\text{droplet}} = 1.728 \cdot 10^{-3} \mu\text{l}$ . Besides the volume, we also have to define at which times the droplets appear at the input channels of the trapping well (i.e. c1 and c6). Therefore, we define a time interval  $\Delta t = 0.1\text{s}$ , which specifies the period at which droplets occur at the input channels of the corresponding droplet streams and flow towards the trapping well. In our considerations (and in order to illustrate the impact of different fluids), we assume that two different fluid settings as given in Tab. II are used, i.e., F1 and F2. For both fluid settings the dynamic viscosity of the continuous phase  $\mu_c$ , and the dispersed phase  $\mu_d$  as well as the density of the continuous phase  $\rho_c$  and the interfacial-tension  $\gamma$  are provided. The used fluids for the continuous phase of the fluid settings F1 and F2 are silicon oils and are also taken from [9]. Moreover, the fluid for the dispersed phase is in both cases ultra-pure water. These different fluid settings are considered in the remainder of this work.

Finally, the objectives of the network have to be specified. If these initial objectives are satisfied (according to the conducted simulations), the respective simulation run is marked “success”. The total number of “success” simulations eventually is used to determine the robustness values.

**Example 5.** The objectives of the trapping well can be easily obtained from its working principles described in Sec. II-C (cf. Fig. 2). More precisely, the following issues are important here:

- If a droplet reaches a trapping well, which is not yet occupied, it has to flow into the corresponding trap.
- If a droplet reaches a trapping well, which is already occupied, it has to flow through the bypass channel (channel c5 or c10) towards the next trapping well.
- If a droplet is already inside a trap it must not be squeezed

through any gap.

If any of these objectives is not satisfied, the network does not work as intended. The network is considered robust if this never happens even if defects according to the considered robustness model exist.

Having all that, robustness analysis can be conducted as outlined in the following for the two robustness models.

1) *Analysis Assuming the Single-Defect-Model:* The single-defect-model considers a single defect of a channel and/or pump, while all other channels/pumps are assumed to be defect-free. In order to determine the minimal and maximal values of all defects, so that the objectives of the network are still satisfied, each dimension (i.e. length, width, height) of all channels and all supply forces of the pumps (i.e. pressure drop and/or volumetric flow rate) are separately considered. More precisely, their respective values are in-/decreased until the objectives of the microfluidic network are no longer satisfied.

It is not possible for a minimal defect to reach values smaller than 0.0, which would lead to a negative parameter<sup>5</sup>. Vice versa, there is no point in increasing the maximal defect as large as possible. Therefore, we defined bounds of the minimal and maximal defect by 0.5 and 2.0, respectively. The motivation behind these limits is that it is very unlikely for defects to change the dimensions of a channel by the factor 0.5 or 2.0, or that pumps fluctuate in such a wide range. If such large deviations occur, something is probably wrong with the fabrication process or the pumps<sup>6</sup>. Thus, we consider the corresponding dimension and pump as robust, when the defect can reach the values 0.5 and 2.0, without harming the objectives of the network. Moreover, the simulation is faster, if the limits for the minimal/maximal defects are not too large, because a smaller search space has to be considered.

**Example 6.** Consider again the running example as well as the settings and constraints discussed in Examples 3, 4, and 5. Furthermore, assume the minimal value for the defect of the height of the channel c5 should be determined, i.e.,  $\Delta_{\min}(h_{c5})$ . When considering the lower bound of 0.5, the defect can reach values from  $0.5 < \Delta_{\min}(h_{c5}) < 1.0$ , which also defines the search space. In order to determine the actual value for  $\Delta_{\min}(h_{c5})$ , a start value has to be defined; for example the middle of the interval  $\Delta_{\min}(h_{c5}) = 0.75$ . This defect value is multiplied by the initial height  $h_{c5} = 60\mu\text{m}$  of the channel, in order to get the defect-height  $h_{c5,\text{defect}} = \Delta_{\min}(h_{c5}) \cdot h_{c5} = 45\mu\text{m}$ . Using

<sup>5</sup>Please note that defect values are always relative values with respect to the initial value.

<sup>6</sup>Of course, these bounds can always be revised according to the designer’s experience.

the simulator with this updated value allows us to check whether the objectives of the network are still satisfied. If the objectives are not satisfied anymore, the defect was too large and, therefore, we have to search the defect value in between  $0.75 < \Delta_{\min}(h_{c5}) < 1.0$ . Otherwise, the defect value lies in between  $0.5 < \Delta_{\min}(h_{c5}) < 0.75$ . This search process can now be repeated, until a desired accuracy is reached, which can also be specified by the designer. Similar, the maximal defect of the height  $\Delta_{\max}(h_{c5})$  can be found with a search process between the initial value and the upper bound defect limit, i.e.,  $1.0 < \Delta_{\max}(h_{c5}) < 2.0$ .

2) *Analysis Assuming the Multi-Defect-Model:* The multi-defect-model assumes multiple defects on all channels/pumps in the network, which allows to consider defect combinations. As discussed in Sec. IV-B, this model does not consider minimal/maximal defect limits as the single-defect-model, but considers the injection of multiple defects—determined by a normal Gaussian distribution with a certain standard deviation.

Such defects are generated for all dimensions of each channel as well as for all pumps<sup>7</sup>. After applying all random defects to the network, the simulation starts. Next, the results of the simulation are compared with the initial objectives and, if they are satisfied, the simulation is marked “success”. This entire process is repeated  $N$  times—every time with different random defects that share the same standard deviation. In other words, a so-called Monte-Carlo-Simulation is conducted. The number of “success” simulations divided by the number of total simulations eventually yields the robustness value. More precisely, a probability value results that states how likely it is to fabricate a microfluidic network, which does work as intended.

**Example 7.** *Once more, consider the running example with the settings and constraints discussed in Examples 3, 4, and 5. Moreover, assume that  $N = 20\,000$  simulations are conducted, where each simulation considers defects according to a normal Gaussian distribution with mean  $\mu = 1.0$  and standard deviation  $\sigma = 0.15$ .  $N_{\text{Success}} = 18\,670$  simulations fulfilled the initial objectives and are marked as “success”. Therefore, we are able to calculate a probability value of*

$$p_{\text{Success}} = \frac{N_{\text{Success}}}{N} = 93.35\% . \quad (7)$$

*This probability value indicates, how likely it is to get a network which does work as intended.*

## VI. RESULTS & DISCUSSION

In this section, we present and discuss the results obtained by the proposed robustness analysis as well as the respectively required computational efforts. To this end, the methods described above have been implemented in Java on top of the open-source simulator provided in [27]. The resulting method has then been evaluated using a single trapping well of the microfluidic network taken from [9] (cf. Sec. II-C)

<sup>7</sup>Of course, the designer can also choose to consider defects in channels only or defects in pumps only.

for which both, detailed specifications and fabrications, are available, as described in Tab. I and Tab. II. The evaluations have been conducted on a regular laptop with an Intel Core i5-8250U @ 1.60/1.80GHz and 8GB RAM running Windows 10. In the following, the obtained results considering the single-defect-model and the multi-defect-model are presented and discussed.

### A. Results of the Single-Defect-Model

In order to conduct a robustness analysis for single defects, we applied the robustness model proposed in Sec. IV-B and the objectives as well as methods discussed in Sec. V. Here, a single defect either on one of the channels or on one of the pumps of the design from Fig. 2 is considered. Furthermore, two different fluid settings (with properties as already summarized in Tab. II and denoted by  $F1$  and  $F2$ ) are considered to additionally evaluate the impact of different fluids. Tab. III summarizes the correspondingly obtained results. Here, each column represents the results obtained for one of the fluid settings. The rows provide the minimal and maximal defect value that is possible for a channel’s width ( $\Delta_{w,\min}$ ,  $\Delta_{w,\max}$ ), height ( $\Delta_{h,\min}$ ,  $\Delta_{h,\max}$ ), and length ( $\Delta_{l,\min}$ ,  $\Delta_{l,\max}$ ) as well as for each of the pumps (i.e.  $\Delta_{\min}$ ,  $\Delta_{\max}$ ), so that the considered objectives are still satisfied. Please note that the defect values in the table represent relative values; in order to get the absolute minimal and maximal values the values from the table have to be multiplied with the given value of the channel dimension or supply force of the pump. Furthermore, as described in Sec. V-B1, the value for the minimal and maximal defect is limited to 0.5 and 2.0, respectively. Channels/pumps which values go beyond this limit are considered very robust with respect to the single-defect-model and, hence, are not explicitly listed in Table III. As a result, only the two gaps (i.e. c4 and c9), the two bypass channels (i.e. c5 and c10) and the two pumps (i.e. p1 and p2) are listed in the table. Since the design of the trapping well is symmetrical, the corresponding channels and pumps also have the same defect values.

This already provides a very helpful result for the designer. In fact, from this, it can be concluded that the design proposed in [9] is already very robust for most of its channels (assuming the single-defect-model). Only the channels c4, c5, c9, and c10 are rather sensitive to fabrication defects and, hence, it is important to have a special focus on these four channels during the fabrication process. Furthermore, it can be observed that the robustness of the network is substantially better for the fluid combination F1 compared to the fluid combination F2. This indicates that the fluid combination F2 is maybe not the best choice for this microfluidic system. As provided in the bottom of Tab. III, the total computational time for the analysis assuming the single-defect-model is 4 seconds for each fluid combination. That is, the data needed to draw these conclusions on the robustness of the network can be determined in negligible time.

### B. Results of the Multi-Defect-Model

In this section, we present the results of the robustness analysis when the multi-defect-model is used (considering the same objectives as before). As discussed above, a

TABLE III: Results obtained with the single-defect-model

	Fluid Settings	
	F1	F2
Channels: c4, c9		
$\Delta_{w,\min}$	0.604	0.604
$\Delta_{w,\max}$	> 2.0	> 2.0
Channels: c5, c10		
$\Delta_{w,\min}$	< 0.5	0.669
$\Delta_{w,\max}$	> 2.0	> 2.0
$\Delta_{h,\min}$	0.523	0.783
$\Delta_{h,\max}$	1.691	1.691
$\Delta_{l,\min}$	< 0.5	< 0.5
$\Delta_{l,\max}$	> 2.0	1.946
Pumps: p1, p2		
$\Delta_{\min}$	0.539	0.539
$\Delta_{\max}$	> 2.0	1.707
Computational		
Time	4 s	4 s

TABLE IV: Accuracy of robustness analysis

	Number of Simulations ( $N$ )					
	10	100	1000	10000	20000	30000
$p_{\text{Success}}[\%]$	60.00	81.00	74.50	75.95	75.80	76.28

Monte-Carlo-Simulation approach is employed for this purpose. Obviously, the accuracy of this strongly depends on the number of conducted simulation runs. Hence, in a first series of evaluations, the effect of the number of runs to the obtained results is considered. To this end, Tab. IV lists the results of the analysis of the multi-defect-model for the fluid combination F1 and defect values based on a normal Gaussian distribution with a standard deviation of  $\sigma = 0.20$ . As it can be observed from the table, the values for  $p_{\text{Success}}$  fluctuate in a wide range for a small number of simulation runs (i.e.  $N \leq 100$ ), while it converges to a certain value of around 76.00% when more simulation runs are conducted. In fact, further increasing the number of simulation runs does not lead to much better/more accurate values which is why we decided to set the number of simulations in the analysis of the multi-defect-model to  $N = 20\,000$ ; a value which yields a sufficient accuracy.

Based on that, a second series of evaluations was conducted to analyze the robustness of the considered design with respect to the multi-defect-model. The correspondingly obtained results are shown in Tab. V. As in the table of the single-defect-model, each column represents the results for one of the fluid settings described above, i.e., F1 and F2. The rows show the success rate  $p_{\text{Success}}$  for different standard deviations. Furthermore, to provide more detailed insights on the impact of defected channels and pumps, we distinguish the results by considering only channels as defect (provided in Tab. Va), only pumps as defect (provided in Tab. Vb), and both as defect (provided in Tab. Vc).

As can be seen from the results, the channels have more impact on the network than the pumps. In fact, from these results, the designer can conclude that defects in the channels might be the most likely cause for unintended behavior in the network. Moreover, the fluid combination F2 always shows a lower success rate than the fluid combination F1, which

correlates with the results from the single-defect-model and, again, indicates that the fluid combination F2 is maybe not the best choice for this microfluidic system. Finally, also a rather general conclusion on the robustness of the design can be drawn: If the designer can ensure a fabrication process and a pump behavior, which yields actual results that do not differ by a maximal standard deviation of  $\sigma = 0.05$ , then there is a good chance that the fabricated design works as expected with the fluid combination F1 (cf. second row of Tab. Vc:  $p_{\text{Success}} = 100\%$ ). In contrast, if the respectively used setup is known to employ deviations of  $\sigma = 0.35$  or more, the chance to obtain a correct working network is only 21.12% for the fluid combination F1. In this case, probably alternative realizations/specifications should be sought. Considering that the variations of fabrication processes is often known<sup>8</sup>, a robustness result such as that can significantly help the designer to decide whether his/her design indeed is robust enough or should be improved. Although the runtime needed to determine the results is substantially larger than for the single-defect-model, 13 minutes of simulation time still is acceptable.

Overall, these evaluations confirmed the benefits of the proposed robustness analysis and showed that corresponding analyses are indeed feasible. It provides designers with a simple metric to decide how sensitive designs for microfluidic networks, corresponding devices such as pumps, or utilized fluids are against defects. This helps designers to improve their microfluidic device, since it allows them to locate critical parts (e.g., channels, pumps, etc.), which have a major impact on the behavior of the device and where the designer have to put a special focus on. Compared to the current state-of-the-art, where no robustness analysis is available at all and designs are determined in a “trial and error”-fashion (i.e. corresponding devices are fabricated and eventually tested; as also done in [9] for the microfluidic network considered here), this constitutes a substantial improvement.

## VII. CONCLUSION

In this work, we proposed models and methods for a robustness analysis of microfluidic networks. This is motivated by the fact that the realization of these devices frequently yields defects caused by fabrication tolerances, pressured induced deformation, swelling of soft structural materials (i.e. PDMS), or fluctuations in the supply force of pumps. This may result in unintended behavior of the network—rendering the network useless. Therefore, designers would like to anticipate the effects and create designs which are robust against those defects. In order to address this, corresponding models and methods have been presented, which allow designers, for the first time, to evaluate the robustness of their microfluidic designs. The proposed models target single defects as well as multiple defects. Finally, the applicability of these models with respect to quality and effort has been demonstrated and discussed. The resulting robustness analysis gives designers important

<sup>8</sup>In fact, often corresponding *correction factors* are employed because of that.

TABLE V: Results obtained with the multi-defect-model

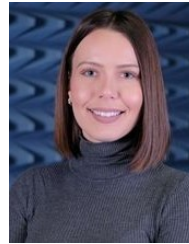
(a) Channels			(b) Pumps			(c) Pumps and channels		
Fluid Settings			Fluid Settings			Fluid Settings		
	F1	F2		F1	F2		F1	F2
$P_{\text{Success}}[\%]$			$P_{\text{Success}}[\%]$			$P_{\text{Success}}[\%]$		
$\sigma = 0.05:$	100.00	100.00	$\sigma = 0.05:$	100.00	100.00	$\sigma = 0.05:$	100.00	99.96
$\sigma = 0.10:$	99.76	94.27	$\sigma = 0.10:$	100.00	100.00	$\sigma = 0.10:$	99.69	92.83
$\sigma = 0.15:$	93.68	75.66	$\sigma = 0.15:$	99.73	99.72	$\sigma = 0.15:$	93.35	73.31
$\sigma = 0.20:$	78.15	53.78	$\sigma = 0.20:$	97.54	97.47	$\sigma = 0.20:$	75.80	52.30
$\sigma = 0.25:$	57.98	36.22	$\sigma = 0.25:$	92.80	92.29	$\sigma = 0.25:$	54.74	33.57
$\sigma = 0.30:$	39.15	22.13	$\sigma = 0.30:$	86.43	85.03	$\sigma = 0.30:$	35.20	19.59
$\sigma = 0.35:$	24.72	13.15	$\sigma = 0.35:$	81.10	77.18	$\sigma = 0.35:$	21.12	11.23
Computational			Computational			Computational		
Time	13 min	13 min	Time	13 min	13 min	Time	13 min	13 min

insights on how to specify their microfluidic networks so that it becomes less affected to physical defects. By this, this work provides a fundamental basis for analyzing the robustness of microfluidic networks with respect to defects in channels and pressure sources. Future work may build up on that by, e.g., addressing further components such as droplet sorting, droplet generation, etc. as well as the support of further defects and characteristics (such as channel roughness).

## REFERENCES

- [1] H. Gu, M. H. Duits, and F. Mugele, "Droplets formation and merging in two-phase flow microfluidics," *International Journal of Molecular Sciences*, vol. 12, no. 4, pp. 2572–2597, 2011.
- [2] S.-Y. Teh, R. Lin, L.-H. Hung, and A. P. Lee, "Droplet microfluidics," *Lab on a Chip*, vol. 8, pp. 198–220, 2008.
- [3] P. Sajeesh, M. Doble, and A. Sen, "Hydrodynamic resistance and mobility of deformable objects in microfluidic channels," *Biomicrofluidics*, vol. 8, no. 5, p. 054112, 2014.
- [4] P. Sajeesh, S. Manasi, M. Doble, and A. Sen, "A microfluidic device with focusing and spacing control for resistance-based sorting of droplets and cells," *Lab on a Chip*, vol. 15, no. 18, pp. 3738–3748, 2015.
- [5] M. Kim, Y. Huang, K. Choi, and C. H. Hidrovo, "The improved resistance of PDMS to pressure-induced deformation and chemical solvent swelling for microfluidic devices," *Microelectronic Engineering*, vol. 124, pp. 66–75, 2014.
- [6] S. K. Sia and G. M. Whitesides, "Microfluidic devices fabricated in poly (dimethylsiloxane) for biological studies," *Electrophoresis*, vol. 24, no. 21, pp. 3563–3576, 2003.
- [7] J. N. Lee, C. Park, and G. M. Whitesides, "Solvent compatibility of poly (dimethylsiloxane)-based microfluidic devices," *Analytical Chemistry*, vol. 75, no. 23, pp. 6544–6554, 2003.
- [8] F. Jousse, G. Lian, R. Janes, and J. Melrose, "Compact model for multiphase liquid–liquid flows in micro-fluidic devices," *Lab on a Chip*, vol. 5, no. 6, pp. 646–656, 2005.
- [9] X. Chen and C. L. Ren, "A microfluidic chip integrated with droplet generation, pairing, trapping, merging, mixing and releasing," *RSC Advances*, vol. 7, no. 27, pp. 16738–16750, 2017.
- [10] Z. Li, K. Y.-T. Lai, J. McCrone, P.-H. Yu, K. Chakrabarty, M. Pajic, T.-Y. Ho, and C.-Y. Lee, "Efficient and adaptive error recovery in a micro-electrode-dot-array digital microfluidic biochip," *Trans. on Computer-Aided Design of Integrated Circuits and Systems*, vol. 37, no. 3, pp. 601–614, 2018.
- [11] C. Liu, B. Li, B. B. Bhattacharya, K. Chakrabarty, T.-Y. Ho, and U. Schlichtmann, "Testing microfluidic fully programmable valve arrays (FPVAs)," in *Design, Automation and Test in Europe*, 2017, pp. 91–96.
- [12] W.-L. Huang, A. Gupta, S. Roy, T.-Y. Ho, and P. Pop, "Fast architecture-level synthesis of fault-tolerant flow-based microfluidic biochips," in *Design, Automation and Test in Europe*, 2017, pp. 1671–1676.
- [13] K. W. Oh, K. Lee, B. Ahn, and E. P. Furlani, "Design of pressure-driven microfluidic networks using electric circuit analogy," *Lab on a Chip*, vol. 12, no. 3, pp. 515–545, 2012.
- [14] G. Cristobal, J.-P. Benoit, M. Joanicot, and A. Ajdari, "Microfluidic bypass for efficient passive regulation of droplet traffic at a junction," *Applied Physics Letters*, vol. 89, no. 3, pp. 34104–34104, 2006.
- [15] T. Glawdel, C. Elbuken, and C. Ren, "Passive droplet trafficking at microfluidic junctions under geometric and flow asymmetries," *Lab on a Chip*, vol. 11, no. 22, pp. 3774–3784, 2011.
- [16] T. Glawdel and C. L. Ren, "Global network design for robust operation of microfluidic droplet generators with pressure-driven flow," *Microfluidics and Nanofluidics*, vol. 13, no. 3, pp. 469–480, 2012.
- [17] M. J. Fuerstman, A. Lai, M. E. Thurlow, S. S. Shevkopyas, H. A. Stone, and G. M. Whitesides, "The pressure drop along rectangular microchannels containing bubbles," *Lab on a Chip*, vol. 7, no. 11, pp. 1479–1489, 2007.
- [18] A. Biral and A. Zanella, "Introducing purely hydrodynamic networking functionalities into microfluidic systems," *Nano Communication Networks*, vol. 4, no. 4, pp. 205–215, 2013.
- [19] E. De Leo, L. Galluccio, A. Lombardo, and G. Morabito, "Networked labs-on-a-chip (NLoC): Introducing networking technologies in microfluidic systems," *Nano Communication Networks*, vol. 3, no. 4, pp. 217–228, 2012.
- [20] A. Grimmer, W. Haselmayr, A. Springer, and R. Wille, "A discrete model for Networked Labs-on-Chips: Linking the physical world to design automation," in *Design Automation Conference*, 2017, pp. 50:1–50:6.
- [21] A. Grimmer, W. Haselmayr, and R. Wille, "Automatic droplet sequence generation for microfluidic networks with passive droplet routing," *Trans. on Computer-Aided Design of Integrated Circuits and Systems*, 2018.
- [22] K. Churski, M. Nowacki, P. M. Korczyk, and P. Garstecki, "Simple modular systems for generation of droplets on demand," *Lab on a Chip*, vol. 13, no. 18, pp. 3689–3697, 2013.
- [23] M. Hamidovic, W. Haselmayr, A. Grimmer, and R. Wille, "Droplet-on-demand for realizing flexible and programmable lab-on-chip devices," in *Int'l Conf. on Miniaturized Systems for Chemistry and Life Sciences*, 2018.
- [24] M. Hamidović, W. Haselmayr, A. Grimmer, R. Wille, and A. Springer, "Passive droplet control in microfluidic networks: A survey and new perspectives on their practical realization," *Nano Communication Networks*, vol. 19, pp. 33–46, 2019.
- [25] M. Schindler and A. Ajdari, "Droplet traffic in microfluidic networks: A simple model for understanding and designing," *Physical Review Letters*, vol. 100, no. 4, p. 044501, 2008.
- [26] H. Bruus, *Theoretical microfluidics*. Oxford university press Oxford, 2008, vol. 18.
- [27] A. Grimmer, M. Hamidović, W. Haselmayr, and R. Wille, "Advanced simulation of droplet microfluidics," *Journal on Emerging Technologies in Computing Systems*, vol. 15, no. 3, p. 26, 2019, a simply version of the simulator is online available at [http://iic.jku.at/eda/research/microfluidics\\_simulation/](http://iic.jku.at/eda/research/microfluidics_simulation/).
- [28] M. G. Simon, R. Lin, J. S. Fisher, and A. P. Lee, "A laplace pressure based microfluidic trap for passive droplet trapping and controlled release," *Biomicrofluidics*, vol. 6, no. 1, p. 014110, 2012.
- [29] A. Grimmer, X. Chen, M. Hamidović, W. Haselmayr, C. L. Ren, and R. Wille, "Simulation before fabrication: a case study on the utilization of simulators for the design of droplet microfluidic networks," *RSC Advances*, vol. 8, pp. 34733–34742, 2018. [Online]. Available: <http://dx.doi.org/10.1039/C8RA05531A>

- [30] A. Grimmer, W. Haselmayr, and R. Wille, "Automated dimensioning of Networked Labs-on-Chip," *Trans. on Computer-Aided Design of Integrated Circuits and Systems*, 2018.
- [31] A. Grimmer, P. Frank, P. Ebner, S. Häfner, A. Richter, and R. Wille, "Meander designer: Automatically generating meander channel designs," *Micromachines – Journal of Micro/Nano Sciences, Devices and Applications*, vol. 9, no. 12, 2018.
- [32] W. Haselmayr, A. Biral, A. Grimmer, A. Zanella, A. Springer, and R. Wille, "Addressing multiple nodes in Networked Labs-on-Chips without payload re-injection," in *Int'l Conf. on Communications*, 2017.
- [33] J. H. Patel, "Stuck-at fault: a fault model for the next millennium," in *Proceedings International Test Conference 1998 (IEEE Cat. No. 98CH36270)*. IEEE, 1998, p. 1166.
- [34] G. L. Smith, "Model for delay faults based upon paths." in *ITC*, 1985, pp. 342–351.
- [35] S. Huhn, S. Frehse, R. Wille, and R. Drechsler, "Determining application-specific knowledge for improving robustness of sequential circuits," *Trans. on Very Large Scale Integration Systems*, vol. 27, no. 4, pp. 875–887, 2019.
- [36] L. Doyen, T. A. Henzinger, A. Legay, and D. Nickovic, "Robustness of sequential circuits," in *2010 10th International Conference on Application of Concurrency to System Design*. IEEE, 2010, pp. 77–84.
- [37] G. Fey, A. Sulflow, S. Frehse, and R. Drechsler, "Effective robustness analysis using bounded model checking techniques," *Trans. on Computer-Aided Design of Integrated Circuits and Systems*, vol. 30, no. 8, pp. 1239–1252, 2011.
- [38] R. Drechsler, S. Eggersgluss, G. Fey, A. Glowatz, F. Hapke, J. Schlöffel, and D. Tille, "On acceleration of SAT-based ATPG for industrial designs," *Trans. on Computer-Aided Design of Integrated Circuits and Systems*, vol. 27, no. 7, pp. 1329–1333, 2008.
- [39] S. Eggersgluß, R. Wille, and R. Drechsler, "Improved SAT-based ATPG: More constraints, better compaction," in *Int'l Conf. on Computer-Aided Design*. IEEE Press, 2013, pp. 85–90.
- [40] T. Glatzel, C. Litterst, C. Cupelli, T. Lindemann, C. Moosmann, R. Niekrawietz, W. Streule, R. Zengerle, and P. Koltay, "Computational fluid dynamics (CFD) software tools for microfluidic applications—a case study," *Computers & Fluids*, vol. 37, no. 3, pp. 218–235, 2008.
- [41] M. Wörner, "Numerical modeling of multiphase flows in microfluidics and micro process engineering: a review of methods and applications," *Microfluidics and Nanofluidics*, vol. 12, no. 6, pp. 841–886, 2012.



idic networks.

**Medina Hamidović** has received her B.Sc. degree in electrical engineering at the University of Tuzla in 2014. In 2017, Hamidović received her joint Master's degree in electrical engineering from Heriot-Watt University (UK), University of South-East Norway and Budapest University of Technology and Economics. At the moment, Hamidović is a Ph.D. researcher at the Institute for Communications Engineering and RF-Systems at the Johannes Kepler University Linz (Austria). Her research is focused on the area of molecular communications and microflu-



**Werner Haselmayr** (S'08—M'13) received the Dipl.-Ing. degree in telematics from the Graz University of Technology, Austria and the Dr. techn. degree in mechatronics from the Johannes Kepler University Linz, Austria, in 2007 and 2013, respectively. He is currently an Assistant Professor at the Institute for Communications Engineering and RF-Systems at Johannes Kepler University. His research interests include algorithm design for wireless communications, iterative processing and molecular communication.



**Gerold Fink** received the Master's degree in mechatronics from the Johannes Kepler University Linz, Austria, in 2019. Currently, he is a Ph.D. student at the Institute of Integrated Circuits at the Johannes Kepler University. His research area focuses on simulations and design automations for microfluidic networks.



**Robert Wille** (M'06–SM'15) is Full Professor at the Johannes Kepler University Linz, Austria. He received the Diploma and Dr.-Ing. degrees in Computer Science from the University of Bremen, Germany, in 2006 and 2009, respectively. Since then, he worked at the University of Bremen, the German Research Center for Artificial Intelligence (DFKI), the University of Applied Science of Bremen, the University of Potsdam, and the Technical University Dresden. Since 2015, he is working in Linz. His research interests are in the design of circuits and

systems for both conventional and emerging technologies. In these areas, he published more than 250 papers in journals and conferences and served in editorial boards and program committees of numerous journals/conferences such as TCAD, ASP-DAC, DAC, DATE, and ICCAD. For his research, he was awarded, e.g., with a Best Paper Award at ICCAD, a DAC Under-40 Innovator Award, a Google Research Award, and more.



**Andreas Grimmer** received the Master degree (2015) as well as Dr. techn. degree (2019) in computer science from the Johannes Kepler University, Austria. Since 2019, he is a Technology Strategist at Dynatrace. His work and research focus on cloud-native technology and techniques that enhance continuous delivery and continuous operation.